Review

International Journal of Modern Physics B
Vol. 23, No. 15 (2009) 3195–3204

World Scientific
www.worldscientific.com

POLARIZED ATOMIC FERMI GASES

WENHUI LI*, G. B. PARTRIDGE†, Y. A. LIAO‡ and R. G. HULET§

Department of Physics and Astronomy and Rice Quantum Institute, Rice University, 6100 Main St., Houston TX 77005, USA

**wenhui.li@nus.edu.sg*

†*guthrie.partridge@institutoptique.fr*

‡*yaliao@rice.edu*

§*randy@rice.edu*

Received 1 June 2009

We review recent experimental studies on polarized atomic Fermi gases. The particular focus is on our own experiments of strongly interacting two-component Fermi gases with imbalanced populations. The real-space density distributions reveal a superfluid/normal phase separation at very low temperatures, accompanied by deformation of evenly paired core; at higher temperatures, a partially polarized phase is observed.

Keywords: Atomic Fermi gases; polarized; phase diagram.

1. Introduction

In fermionic systems, the formation of pairs between two constituent components is the essential ingredient for fascinating macroscopic quantum phenomena of superfluidity and superconductivity, which result from the condensation of those fermion pairs. The characteristics of fermion pairs and the properties of their condensates strongly depend on the coupling strength and the Fermi energies of two components. In ultracold atomic systems, all these parameters are widely tunable and highly controllable, therefore experimental studies of fermionic atoms offer a unique opportunity in understanding fermionic pairing and related phenomena such as high T_c superconductivity, and perhaps even more exotic quark pairing in nucleons and neutron stars. During the past few years, there has been impressive progress in exploring pairing of ultracold fermionic atoms. As the interaction between two pairing components increases from weak to strong, the condensate goes smoothly from a Bardeen–Cooper–Schrieffer (BCS) like superfluid of spatially large correlated pairs,

*Current address: Center for Quantum Technologies, National University of Singapore, 3 Science Drive 2, Singapore, 117543.

†Current address: Laboratoire Charles Fabry de l'Institue d'Optique, UMR CNRS 8501, Palaiseeau, France.

applicable to conventional superconductors, to Bose–Einstein condensation (BEC) of tightly-bound bosonic diatomic molecules. This so-called "BCS-BEC crossover" has been explored by several groups in ultracold atomic gases of two-spin-state mixture[1–7] by use of a magnetically-tuned Feshbach resonance to change interaction. These experiments have advanced our understanding of the strongly interacting regime lying between these two extremes.

Another opportunity opened up by experiments with ultracold atoms is the study of possible pairing mechanisms and corresponding phases in systems with mismatched Fermi energies. As early as 1960's, not long after the BCS theory was established, the question whether superfluid may sustain with different Fermi energies has already arisen. The two particularly interesting phases being proposed for the mismatched case are the FFLO state (the initials of the originators of the idea) with pairing of non-zero center-of-mass momentum,[8,9] and the deformed Fermi surface (DFS) state[10] where the local Fermi surfaces of two components deform from being spherical to maximize their overlap. Both of these phases correspond to broken space symmetries. Other possible phases include the polarized superfluid,[11,12] and phase separation for paring of strong interaction.[13–17] Experimental confirmation of these exotic phases in condensed matter systems has remained elusive because of the fundamental incompatibility between magnetism and superconductivity. In contrast, it is relatively straightforward to create an atomic Fermi gas of mismatched Fermi energies either with unequal numbers of two spin states or with two different atomic species (different masses). Experimental investigations of Fermi gases with imbalanced populations have been conducted by groups at MIT and Rice.[18–21]

In this paper, we review our experiments at Rice on a strongly interacting polarized Fermi gas of ^{6}Li atoms. The main results of our experiments are the observation of phase separation between a fully paired superfluid core and unpaired excess atoms surrounding the core, the deformation of the core due to surface tension at the superfluid/normal interface, and the temperature dependence of the phases.

2. General Methods

Our methods for producing a two-component degenerate Fermi gas with imbalanced populations have been discussed in several previous publications.[7,19,20] Atoms of both isotopes of lithium, bosonic ^{7}Li, and fermionic ^{6}Li, out of a Zeeman slower are loaded into a magneto-optical trap, and then transferred to an Ioffe-Pritchard magnetic trap with a clover-leaf configuration, where they are cooled by rf evaporation. Since spin symmetry prevents spin-polarized fermionic ^{6}Li atoms from undergoing *s*-wave collisions, the simultaneously trapped and cooled ^{7}Li atoms function as a thermal reservoir to cool the ^{6}Li atoms. During the dual evaporation, two rf frequencies are used to remove the most energetic ^{7}Li and ^{6}Li atoms, respectively, and the remaining ^{7}Li atoms rethermalize through collisions among themselves, while the ^{6}Li atoms rethermalize through collisions with the ^{7}Li atoms.

There is a broad Feshbach resonance between the two lowest hyperfine states $F = 1/2$, $m_F = 1/2$ (state $|1\rangle$) and $F = 1/2$, $m_F = -1/2$ (state $|2\rangle$) at 834 G.[22,23] However, neither of the states is magnetically trappable. To utilize this Feshbach resonance for tuning interaction, at the end of evaporation in the magnetic trap, the ^{6}Li atoms in the doubly polarized state $F = 3/2$, $m_F = 3/2$ are transferred to an optical trap formed from a single focused infrared laser beam operating at wavelength of 1080 nm. A single rf sweep in a nearly uniform bias field of 754 G then transfers atoms to state $|1\rangle$. Typically 3×10^6 atoms in state $|1\rangle$ at a temperature $T \approx 6$ μK are confined in the optical trap. Since in Fermi-Dirac statistics, only fermions in different quantum states can interact via an s-wave, an *incoherent* spin mixture of state $|1\rangle$ and state $|2\rangle$ is necessary. To ensure the complete decoherence in population transfer, a series of 100 saw-tooth frequency ramps are swept through the rf transition resonance between the two states for 1 s in a magnetic field with weak inhomogeneity. The number of atoms being transferred from state $|1\rangle$ to state $|2\rangle$ can be controlled by rf power, so either even or uneven spin mixture is produced. After preparation of the spin mixture, the atoms are evaporatively cooled by reducing the optical trap depth over a period of approximately 1 s. Thermalization is achieved through collisions between atoms from the two different states. In the middle of evaporation, we adiabatically sweep the magnetic field to the resonance field 834 G, where the s-wave scattering length diverges. The temperature of the gas can be controlled by evaporating to different final trap depths U_0.

At the end of evaporation, states $|1\rangle$ and $|2\rangle$ are sequentially and independently imaged in the trap by absorption using a probe laser beam on resonance with the $2^2S_{1/2}$ to $2^2P_{3/2}$ atomic transitions specific to each state. The two probes are each 3 μs in duration and are separated in time by 27 μs. The separation is minimized to prevent probe-induced broadening of the second image.[19] The numbers of the two states, N_1 and N_2, and the global polarization $P = (N_1 - N_2)/(N_1 + N_2)$, (between 0 and 1), are obtained from analyzing these images. The temperature of the gas is evaluated by fitting the profiles of gases deliberately prepared as $P = 0$ to fermionic non-zero-temperature Thomas–Fermi distributions. $\widetilde{T}$, the fitted temperature, is expected to be closely related to the actual temperature.[5]

3. Results

3.1. *Phase separation and deformation*

Shown in Fig. 1 are a series of images corresponding to a range of P from 0 to 0.95 at $\widetilde{T} \leq 0.05\ T_F$. The first row of each image set corresponds to state $|1\rangle$, the second row, state $|2\rangle$, while the third row is the difference distribution, obtained by subtracting the minority state $|2\rangle$ from the majority state $|1\rangle$. All the essential information of the polarized gases in this work can be extracted from these images. Before discussing the quantitative analysis of the data, here are qualitative features from examination of the images: evenly paired core, deformation of the core, and sharp boundaries. The difference distribution of $P = 0$ case, the usual even spin

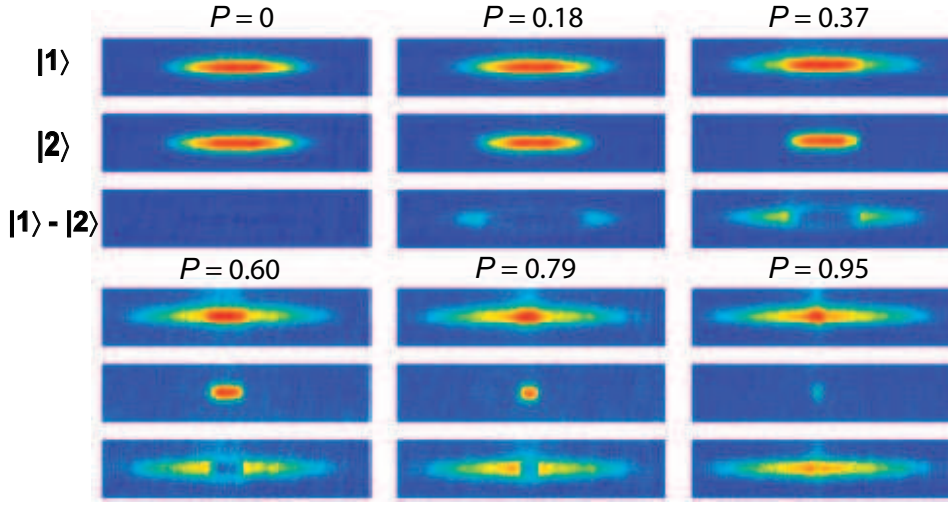

Fig. 1. *In-situ* absorption images of polarized Fermi gases. The field of view for these images is 1654 μm by 81 μm. The displayed aspect ratio is reduced by a factor of 4.4 for clarity. Modified from Fig. 1 in Ref. 20.

mixture, is zero as expected. In the cases of $P \neq 0$, a dark central core in the difference distribution indicates that the column densities of both spin states are nearly equal. Since the radial dimensions of the two states are nearly the same, we can deduce that their real 3D densities are also nearly equal in this core region. This suggests that the distribution of state $|2\rangle$ corresponds to that of the evenly paired core, and that the difference distribution corresponds to the excess unpaired atoms that surround the central core. The striking observation is that the core, instead of assuming the shape of the underlying harmonic trap, becomes highly deformed with increasing P, while the polarized shell is rather concentrated at the axial poles, instead of uniformly surrounding the core. Finally, the boundary between the core and the polarized shell seems quite sharp from the images. All these features together suggest a phase separation between the evenly paired superfluid core and the fully polarized normal phase.

To verify that the core is evenly paired, the 3-dimensional (3D) real-space density distributions are reconstructed from the column densities using the Abel transform.[24] The cylindrical symmetry of distributions is the only requirement of the method, and is fulfilled by our single-beam optical trap. Figure 2 shows an example of a 3D density cut along the trap center line. The boundary between the core and the fully polarized shell is very thin as shown. The difference distribution shows that the central density difference is indeed zero, as asserted previously. The ratio of the 3D central densities of the two spin states is plotted versus P in Fig. 3(a). The central density ratio is approximately equal to unity for all but the highest polarizations, and is totally different from that of a polarized gas in a non-interacting normal case (dotted line). This result is somewhat unexpected, as it shows that

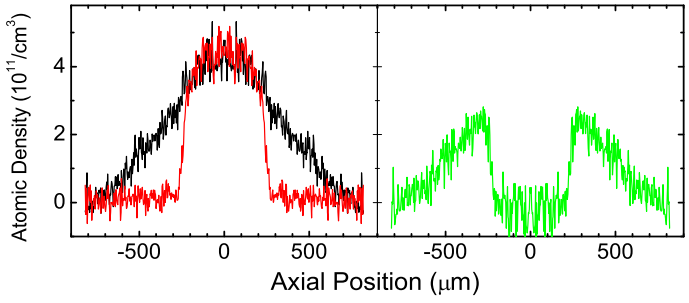

Fig. 2. (Color on line) Center line axial cuts of the reconstructed 3D densities for $P = 0.35$. The black line corresponds to state $|1\rangle$, the red to state $|2\rangle$, the green to their difference. Modified from Fig. 3 in Ref. 20.

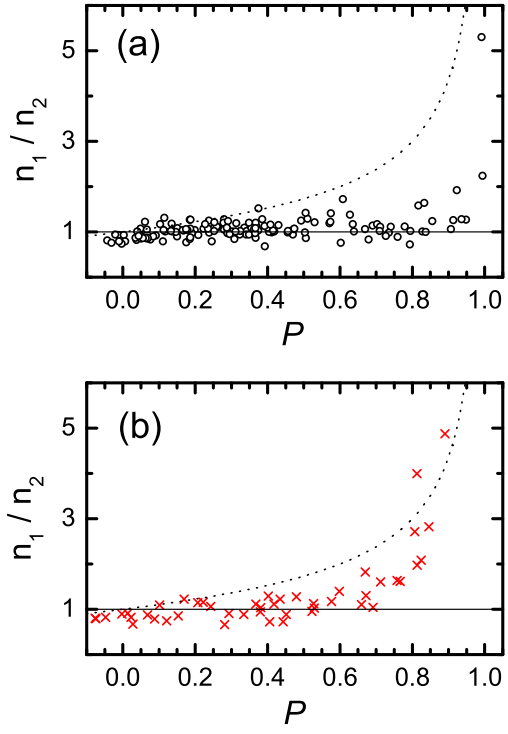

Fig. 3. Ratio of central densities versus P. (a) $\widetilde{T} \leq 0.05\ T_F$; (b) $\widetilde{T} \approx 0.2\ T_F$. The dotted lines correspond to $[(1+P)/(1-P)]^{1/2}$, the expected central density ratio for a harmonically confined, non-interacting gas at $T = 0$. Modified from Fig. 4 in Ref. 20.

phase separation is occurring in this system even above the so-called Clogston limit, where the difference in chemical potentials exceeds the superconducting gap, Δ,[25] and the system will consequently lose any superfluidity. A possible explanation of this discrepancy is that the large aspect ratio of our trapping geometry facilitates pairing at large P.

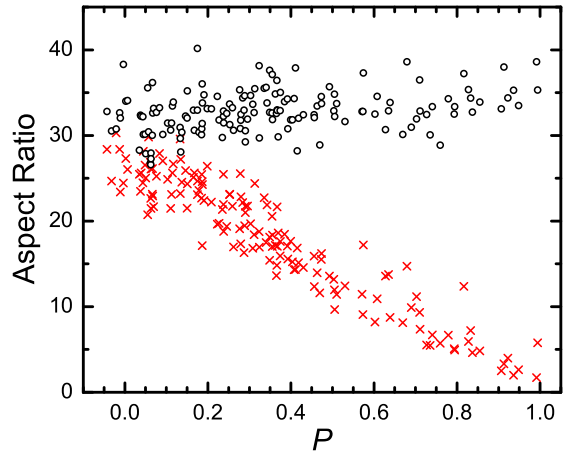

Fig. 4. Aspect ratio versus P. The black circles correspond to state $|1\rangle$, and the red circles, state $|2\rangle$. Reprinted from Fig. 2 in Ref. 20.

To quantify the deformation of the core, the aspect ratios, R_z/R_r, for both states are plotted versus P in Fig. 4. This data clearly shows that the aspect ratio of state $|2\rangle$ (representing an evenly paired core) decreases by an order of magnitude when going from completely unpolarized ($P = 0$) to nearly fully polarized ($P = 0.95$), while that of state $|1\rangle$ changes little through all P from the value given by the trap. This deformation is in violation of local density approximation (LDA), and has been explained by surface tension at the superfluid/normal boundary.[26,27] Haque and Stoof fit the data to a generalized model that includes surface tension.[20,28] With the argument that the Fermi energy E_F is the only energy scale at unitarity limit and the surface energy must be proportional to it within a numerical factor of order unity, they find that the best fit, for all P, corresponds to a constant of proportionality of 0.6.[28] Figure 5 shows a representative fit to a column density cut for $P = 0.35$. The remarkably good fit strongly supports that surface tension is likely the correct explanation for the deformation.

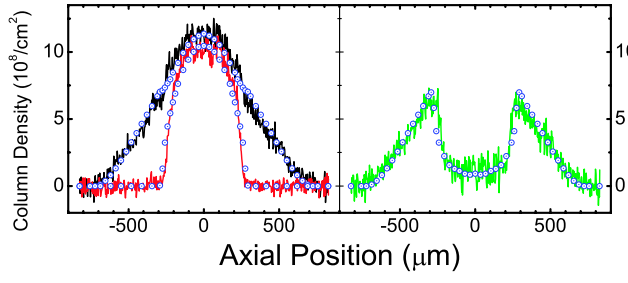

Fig. 5. (Color on line) Column density profiles for $P = 0.35$. The black line corresponds to state $|1\rangle$, the red to state $|2\rangle$, the green to their difference. The circles are the results of a fit to a general model including surface tension. Modified from Fig. 3 in Ref. 20.

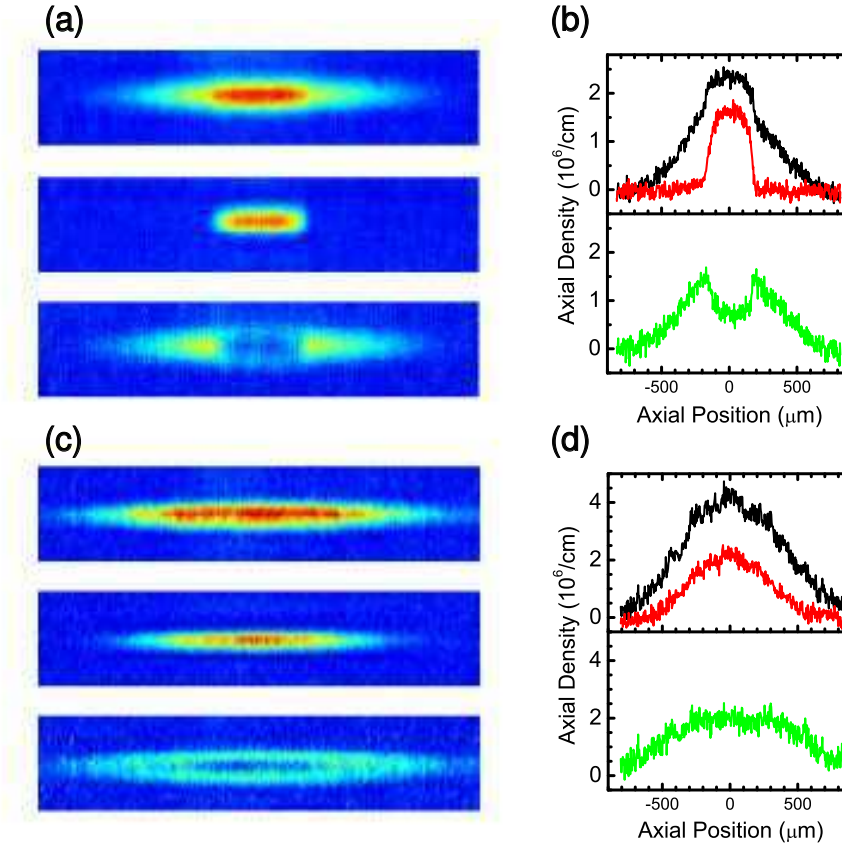

Fig. 6. Absorption images and integrated profiles for (a), (b): $P = 0.5$, $\widetilde{T} \leq 0.05\ T_F$; (c), (d): $P = 0.45$, $\widetilde{T} \approx 0.2\ T_F$. Reprinted from Fig. 5 in Ref. 20.

3.2. *Finite temperature observations*

All of the preceding data correspond to our lowest temperatures, $\widetilde{T} \leq 0.05\ T_F$. (Because of the inherent insensitivity of degenerate Fermi distributions to temperature, only this upper estimate for our coldest distributions can be obtained.) At higher temperatures, polarized Fermi gases behave completely different from at the lowest temperatures. Shown in Figs. 6(a) and 6(c) are absorption images of the lowest ($\widetilde{T} \leq 0.05\ T_F$) and higher ($\widetilde{T} \approx 0.2\ T_F$) temperatures. It is apparent that the density distributions of the two components of the higher temperature gas show no deformation, in contrast to those of the colder case, and the aspect ratios of both state $|1\rangle$ and $|2\rangle$ remain constant and equal, independent of P. We also extracted the ratio of the central densities of the two states, $n_1(0,0)/n_2(0,0)$, for this higher temperature data, and plot it versus P in Fig. 3(b). The central region remains equally paired up to $P \approx 0.6 - 0.7$, indicating that the central region is still superfluid at this temperature. At higher P, the central density ratio for this

higher temperature data is consistent with that of a normal gas. Moreover, the higher temperature data does not exhibit the sharp phase boundary between the central core and the normal region, observed at lower temperatures.

At temperature $\widetilde{T} \approx 0.1\ T_F$, we found that phase separation occurs only for $P > P_c$, where $P_c \approx 0.1$[19]; for $P < P_c$, the observations are consistent with a non-phase-separated polarized superfluid. These results support the suggestion of a temperature dependent transition between a low-temperature phase separated state and a higher temperature polarized superfluid[30,31] as discussed in the following paragraphs.

3.3. *Discussion*

Phase separation was first suggested by Bedaque *et al.*,[13] and was further explored theoretically by several other groups.[14–17,29] A phase separated region appears prominently in all proposed phase diagrams. There have been several proposed phase diagrams at unitarity limit containing a tricritical point.[30–32] Figure 7 shows a proposed phase diagram relevant to a trap where the density distribution is inhomogeneous.[31] The phase diagram contains two superfluid regions — a lower T phase corresponding to phase separation and a higher T polarized superfluid, and a normal phase. The intersection point of the three phases is a tricritical point. The dashed lines indicate qualitatively where our data fit in this diagram. The phase diagram of Fig. 7 agrees well with the data: at low T there is a phase separation at nearly all P and the first-order phase boundary results in sharp interfaces, as observed; at higher T above tricritical point and the transition from the central superfluid to the outer normal phase is smooth, as expected for a second-order phase transition. The data at $\widetilde{T} \approx 0.1\ T_F$ from our prior work[19] is qualitatively consistent

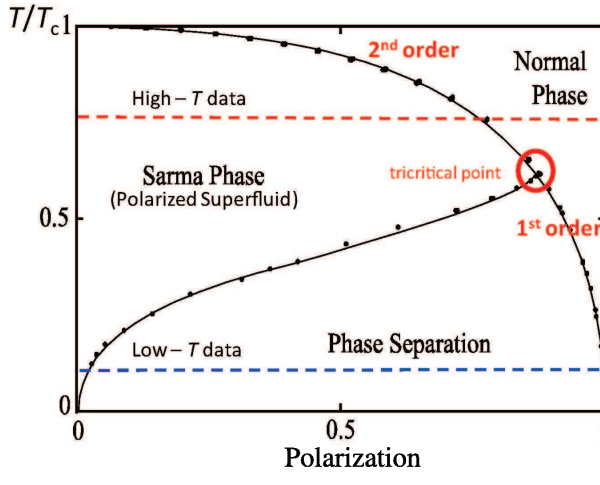

Fig. 7. Proposed phase diagram at unitary. Dashed lines indicate qualitatively where the low and high-T data from Fig. 4. Modified from Ref. 31.

with an intermediate temperature below the tricritical point. The MIT group has recently obtained a phase diagram with a tricritical point for homogeneous gas at unitarity limit.[21] Instead of phase separation through all P, their observations have the Clogston limit at $P = 0.36$ at zero temperature, beyond which the polarized gas goes into normal phase.

4. Conclusion

Ultracold atomic Fermi gases are fascinating for systematic investigations of pairing because of the ability to tune their physical parameters, including interaction strength, polarization, and temperature. They offer clean and controllable experimental systems to study states of matter of relevance to other areas of physics. We have presented a review of our experiments on strongly-interacting two-component Fermi gases with unequal spin populations. At the lowest temperatures the polarized gas phase separates into an evenly paired superfluid core surrounded by a fully polarized shell. Surface tension at the phase boundary results in a marked deformation of the core. At elevated, though, still degenerate temperatures, the observed distributions are consistent with a polarized superfluid, containing an evenly paired central region with gradually increasing polarization along radius. These observations are in agreement with proposed phase diagrams containing two superfluid phases and a tricritical point.

Acknowledgment

We thank H. T. C. Stoof for helpful discussions, and E. Mueller for helpful discussion and for providing the Abel transform code. This research is supported by the NSF, NASA, ONR, and the Welch Foundation.

References

1. C. A. Regal, M. Grenier and D. S. Jin, *Phys. Rev. Lett.* **92**, 040403 (2004).
2. M. W. Zwierlein, C. A. Stan, C. H. Schunck, S. M. F. Raupach, A. J. Kerman and W. Ketterle, *Phys. Rev. Lett.* **92**, 120403 (2004).
3. J. Kinast, S. L. Hemmer, M. E. Gehm, A. Turlapov and J. E. Thomas, *Phys. Rev. Lett.* **92**, 150402 (2004).
4. M. Bartenstein, A. Altmeyer, S. Riedl, S. Jochim, C. Chin, J. Hecker Denschlag and R. Grimm, *Phys. Rev. Lett.* **92**, 120401 (2004).
5. J. Kinast, A. Turlapov, J. E. Thomas, Q. Chen, J. Stajic and K. Levin, *Science* **307**, 1296 (2005).
6. M. W. Zwierlein, J. R. Abo-Shaeer, A. Schirotzek, C. H. Schunck and W. Ketterle, *Nature* **435**, 1047 (2005).
7. G. B. Partridge, K. E. Strecker, R. I. Kamar, M. W. Jack and R. G. Hulet, *Phys. Rev. Lett.* **95**, 020404 (2005).
8. P. Fulde and R. A. Ferrell, *Phys. Rev.* **135**, A550 (1964).
9. A. I. Larkin and Y. N. Ovchinnikov, *Sov. Phys. JETP* **20**, 762 (1965).
10. A. Sedrakian, J. Mur-Petit, A. Polls and H. Müther, *Phys. Rev. A* **72**, 013613 (2005).

11. G. Sarma, *J. Phys. Chem. Solids* **24**, 1029 (1963).
12. W. V. Liu and F. Wilczek, *Phys. Rev. Lett.* **90**, 047002 (2003).
13. P. F. Bedaque, H. Caldas and G. Rupak, *Phys. Rev. Lett.* **91**, 247002 (2003).
14. J. Carlson and S. Reddy, *Phys. Rev. Lett.* **95**, 060401 (2005).
15. D. E. Sheedy and L. Radzihovsky, *Phys. Rev. Lett.* **96**, 060401 (2006).
16. Z.-C. Gu, G. Warner and F. Zhou, cond-mat/0603091.
17. H. Hu and X.-J. Liu, *Phys. Rev. A* **73**, 051603(R) (2006).
18. M. W. Zwierlein, A. Schirotzek, C. H. Schunck and W. Ketterle, *Science* **311**, 492 (2006).
19. G. B. Partridge, W. Li, R. I. Kamar, Y. A. Liao and R. G. Hulet, *Science* **311**, 503 (2006).
20. G. B. Partridge, W. Li, Y. A. Liao and R. G. Hulet, *Phys. Rev. Lett.* **97**, 190407 (2006).
21. Y. Shin, C. H. Schunck, A. Schirotzek and W. Ketterle, *Nature* **451**, 689 (2008).
22. M. Houbiers *et al.*, *Phys. Rev. A* **57**, R1497 (1998).
23. M. Bartenstein *et al.*, *Phys. Rev. Lett.* **94**, 103201 (2005).
24. L. M. Smith and S. I. Sudharsanan, *J. Quant. Spec. Rad. Trans.* **39**, 367 (1988).
25. C. Lobo, A. Recati, S. Giorgini and S. Stringari, *Phys. Rev. Lett.* **97**, 200403 (2006).
26. T. N. De Silva and E. J. Muellerr, *Phys. Rev. A* **73**, 051602 (2006).
27. M. Haque and H. T. C. Stoof, *Phys. Rev. A* **74**, 011602(R) (2006).
28. M. Haque and H. T. C. Stoof, *Phys. Rev. Lett.* **98**, 260406 (2007).
29. F. Chevy, *Phys. Rev. Lett.* **96**, 130401 (2006).
30. M. M. Parish, F. M. Marchetti, A. Lamacraft and B. D. Simons, *Nature Phys.* **3**, 124 (2007).
31. K. B. Gubbles, M. W. J. Romans and H. T. C. Stoof, *Phys. Rev. Lett.* **97**, 210402 (2006).
32. C.-C. Chien, Q. Chen, Y. He and K. Levin, *Phys. Rev. A* **74**, 021602(R) (2006).